Index Similarity Assisted Particle Filter for Early Failure Time Prediction with Applications to Turbofan Engines and Compressors

Xiaochuan Li*[1], School of Electrical Engineering and Automation, Hefei University of Technology, Hefei, China. Email: xiaochuan.li@hfut.edu.cn; xiaochuan.li0309@gmail.com;
Tianran Lin[2]: Faculty of Mechanical and automotive engineering, Qingdao university of technology, Qingdao, China. Email: trlin@qut.edu.cn
Yingjie Yang[3]: Faculty of Computing, Engineering and Media, De Montfort University, Leicester, UK. Email: yyang@dmu.ac.uk
David Mba[4]: Creative Computing Institute, University of the Arts London, London, UK. Email: d.mba@arts.ac.uk

Panagiotis Loukopoulos[5]: School of Aerospace, Transport and Manufacturing, Cranfield University, Cranfield, UK. Email: loukopoulospn@gmail.com

***Abstract*—The particle filter (PF) has been widely studied in the prognostics' field due to its ability to deal with nonlinear and non-stationary systems. However, there is no update of the model parameters during the prediction, preventing PF to work in its traditional way to generate accurate long-term predictions. In order to solve this problem, we put forward an improved PF that is based on a novel health index (HI) similarity matching method. This method is employed to search for similar HIs in the training library and construct an optimal "similar HI" for the system under study. Finally, the obtained HI is consistently fed into the PF to deliver precise state-of-health (SoH) estimates. The effectiveness of the proposed PF was validated on the C-MAPSS datasets as well as data collected from an operational reciprocating compressor. We observed that the new similarity matching method demonstrated excellent performance in finding suitable HIs for failure time prediction. We also observed that the proposed PF framework had a superior prognostics performance over the standard PF. We obtained an averaged predictive accuracy of 96% (C-MAPSS data) and 92% (compressor data) when only the first 10% of the degradation data were used. This work highlights the promise of combining index similarity, Procrustes analysis and PF for complementing existing prognostic methods.**

***Index Terms*—Condition monitoring, particle filter, spherical distance, prognostics.**

I. Introduction

PROGNOSTICS and health management (PHM) generally involves two major tasks, namely diagnosis and prognostics (Z. Wu, Zhang, Guo, Ji, & Pecht, 2022). While fault diagnosis can detect and isolate faults that have already appeared, prognostics could have more meanings since the failure time (FT) or remaining useful life (RUL) can be predicted in advance to facilitate maintenance scheduling, which keeps machines having a maximum uptime with a minimum effective maintenance cost. According to recent review paper (Lei et al., 2018), data-driven FT prediction methods include statistical model-based methods such as inverse Gaussian process model and Wiener process model (N. Chen & Tsui, 2013; Paroissin, 2015); Artificial intelligence-based methods such as artificial neural network and regression tree(Razavi-Far, Chakrabarti, Saif, & Zio, 2019; Romeo et al., 2020). Data-driven methods have demonstrated to be effective in taking advantages of measured condition monitoring data for FT prediction. The statistical model-based FT prediction methods describe the degradation process with a mathematical model and update model parameters with new measured data to predict at future times the state evolution. Statistical model-based methods feature strong long-term prediction abilities since they can make full use of prior knowledge and real-time measurements (Lei et al., 2018). Among all stastical model-based techniques, particle filter has been one of the most common and well-proven approach in the prognostics' filed due to its advantages to approximate the future state probability distributions, almost arbitrary distributions can be represented (Q.-b. Zhang, Wang, & Chen, 2019). Other advantages of applying PF in the context of prognostics, according to the literature, include its strong ability to cope with non-Gaussian and nonlinear systems(Moghaddasi & Faraji, 2020); its probabilistic outputs which account for the significant levels of uncertainty inherent in long-term predictions (Javed, Gouriveau, Zerhouni, & Nectoux, 2014); provision of information fusion and its capability to account for the stochasticity of system degradation (Cui, Li, Wang, Zhao, & Wang, 2022), etc. Over the past decade, many PF based prognnostic methods have been applied successfully in the domain of the reliability and safety of systems (Lim, Goh, Tan, & Dutta, 2017; Cui, Wang, Wang, & Ma, 2019; N. Li, Lei, Lin, & Ding, 2015; Qiu, Li, Jiang, & Zhu, 2018). Apart from the aforementioned studies, there are many nonlinear modeling approaches which proved to be successful in modeling systems in various fields (HEDREA & PETRIU, 2021; Teo, Tan, Ooi, & Lin, 2015; Hedrea, Precup, Roman, & Petriu, 2021).

Particle filter recursively updates the conditional probability distribution over the state space of the system's evolution to estimate its degradation level. If PF is to be used for long-term FT prediction, it is firstly reasonable to allow real-time measurements to be available for a certain duration to enable model parameter training and updating. This stage is referred to as the state tracking phase (aka. filtering). After the state tracking phase, predictions of the state evolution are performed over the state space without the presence of new measurements. This stage is referred to as the state prediction phase. The key challenge lies in the second stage is to find methods that are capable of accurately projecting at future times the posterior distribution represented by the current particle population in the absence of new measurements. To address this challenge, two types of solutions have been proposed in the literature: 1) project at future times the current particles population among all possible pathways over the state space; and 2) "generate" future measurements to extend the state tracking phase. The first solution is the most commonly used. Examples of approaches that adopt the particle projection method can be found in (Baraldi, Cadini, Mangili, & Zio, 2013; Qiu et al., 2018; Cheng, Qu, & Qiao, 2017; Jha, Dauphin-Tanguy, & Ould-Bouamama, 2016; X. Li, Yang, Yang, Bennett, Collop, & Mba, 2019). However, these methods unavoidably involve enlarged uncertainty intervals and accumulated errors for long-term FT predictions, which are also considered to be potential issues for any non-deterministic prediction method (Tang, Orchard, Goebel, & Vachtsevanos, 2011). This is mainly due to the fact that the particle weights remain unchanged during prediction. In other words, there is a lack of methodology for the provision of a model parameter updating procedure similar to that appeared in the state tracking phase. To solve this problem, the second solution which relies on "generating" future measurements was proposed. In (Xiongzi, Jinsong, Diyin, & Yingxun, 2012), a LSSVR model was trained to predict the water level observation series prediction which are then used to recursively update the particle weights for system FT estimation. However, the degradation process of industrial facilities is highly nonlinear and complex, which may lead to complex degradation behaviors (e.g. process noise and nonlinear degradation paths), making it difficult to accurately track the evolution of measurements in the context of long-term prediction with a simple machine learning model. Hence the predictive accuracy of the "generated" measurements could not be fully guaranteed. In addition, the

study assumes only one process variable to be unseen for the future. Predictably, the computational cost will be unaffordable when it comes to high-dimensional measurments in industrial facilities. Constructing a prediction model for each sensor information in high-dimensional settings would in turn accumulate the total discripency between the true and predicted measurements, making the method undesirable for real-world senarios. Nevertheless, the abovementioned methods haven't find an optimal solution to provide accurate FT predictions with high robustness by maintaining an accurate probability density function through model parameter updates.

The objective of this study is to develop a particle filter for prognostics that can provide accurate FT predictions by maintaining an accurate probability density function during the state prediction phase. This is achieved by developing a new particle filter in which a novel Spherical and Cosine distance-based index similarity is proposed to find similar degradation trajectories from historical measurements, and the selected degradation trajectories are then treated as "new measurements" to adjust the probability density function prediction. In similarity based prognostics, a reference data base is created with historical failures which are compared with an ongoing case via distance analysis. This method has attracted increasing attention in the era of big data since it requires neither a time-consuming training process nor any hypothesis to build the fault evolution model. Moreover, it predicts the future evolution based on the system's own historical trajectories and hence the complex degradation behaviors can be well represented (X. Yang, Fang, Yang, Mba, & Li, 2019). In addition, it needs only a small amount of historical data to predict the FT (Y. Liu, Hu, & Zhang, 2019). Therefore, the future trajectories determined by the similarity-based prognostic method can be considered as proper "new measurements" to facilitate the PF's state prediction phase. In similarity based prognostics, Euclidean distance-based similarity received the most attention and it has been extensively studied. In (Loukopoulos et al., 2019, 2019), Euclidean distance was employed to facilitate K-nearest neighbors prognostics. In (Z. Liu, Wang, Song, & Cheng, 2017; Wang, Yu, Siegel, & Lee, 2008), historical failures are directly compared with the testing case via Euclidean distance analysis, and the most similar historical case is considered to have equal FT with the testing case. In a recent study, the similarity-based health index curve matching technique was utilized to identify the training instances that share a similar degradation pattern with the test instance whose FT needs to be determined (Yu, Kim, & Mechefske, 2020). But as pointed out by (Y. Liu et al., 2019), the similarity in the spatial direction is often neglected by researchers due to its complexity. Spatial distance or Cosine distance which measures the similarity in the spatial direction is robust to outliers and noises, hence it has received increasing attention in more recent studies. Cosine distance was put forward in (Y. Liu et al., 2019) to improve the FT prediciton of a slotting cutter and was proved to be better than the sole Euclidean distance measure. In a more recent study (S.-J. Zhang, Kang, & Lin, 2021), both Euclidean and Cosine distance was introduced to find historical failures share similar degradation patterns with the on-site component. However, these distance analysis techniques didn't take the weights of similarity at different time instances into consideration, hence may not be sufficient for accurate FT prediction as the most reccent data actually capture the latest degradation trend. To this end, a novel Spherical and Cosine distance-based index similarity matching method is preoposed in this study for the first time, attempting to leverage the advantages of the most recent Cosine distance method in capturing the spatial distance as well as the Spherical distance's ability to take time differences into consideration. We observed that the proposed method can provide more suitable HIs for subsequent prognostic analysis in that the obtained HI shows closer agreement with the failure time compared with the most widely used Euclidean distance. Ideally, having more historical run-to-failure data to enrich the searching library can potentially result in better HIs, thereby improve the accuracy of failure time prediction. However, it is possible that the HI found by the similarity matching method occasionally does not show close agreement with the actual HI, leading to enlarged FT prediction errors. Therefore, a teaching-learning-based optimization (TLBO) method (Rao, Savsani, & Vakharia, 2011), which is a famous method for solving single-value engineering optimization problems, was further adopted to perform a Procrustes analysis, aiming at adjusting the matched HI when needed and reducing the prediction errors.

To summarize, the new ideas of this manuscript with respect to the literature are: a) A new particle filter framework was proposed for FT prediction. Namely, the index similarity method is proposed to be incorporated into the particle filter framework to enable model parameter updates during the state prediction phase, aiming at providing accurate and efficient PDF estimates in the context of long-term predictions. b) A novel spherical and cosine distance-based index similarity matching method was put forward to find proper health indexes from historical measurements. The proposed PF is presented by its application to the prediction of fault evolution and FT of a fleet of turbofan engines and a real-world operational reciprocating compressor. The main contributions of this work are summarized as follows:1) By leveraging the strengths of the novel similarity-based prognostics and particle filter, the proposed framework offers the promise of improving the predictive accuracy and uncertainty level of standard PF. 2) Thanks to the similarity-based prognostics, our method shows promise in long-term FT estimation, showing a good performance at early failure cycles. 3) Unlike existing research, we put forward a new Spherical-Cosine-distance-based similarity matching method. 4) We introduce a Procrustes analysis based on TLBO to complement the proposed similarity-based prognostic methods, further improving its predictive accuracy. 5) We tested the proposed method on both simulation and real-world data.

The remainder of this paper is organized as follows. Section II states the problem to be solved. Section III introduces the index similarity-assisted PF method. In Section IV and V, two case studies regarding turbine engine faults and reciprocating compressor failures are used for validation and comparison. Finally, some conclusions are given in Section VI.

II. Problem Statement

PF involves using a state evolution model to predict the future state of a system:

$$x_k = g\left(x_{k-1}, x_{k-2}, \ldots, x_1\right) + w_k \tag{1}$$

where g represents the state evolution function, x_k denotes the system state at time k, and w_k represents a noise term. In (1) the system evolution is assumed to be a high-order Markov process, which is in line with the assumptions appeared in the literature (C. Chen, Zhang, Vachtsevanos, & Orchard, 2010; X. Li, Yang, Yang, Bennett, Collop, & Mba, 2019), since a first-order Markov process may not always be an appropriate hypothesis (Jouin, Gouriveau, Hissel, Péra, & Zerhouni, 2016) for fault evolution. PF generates a set of particles (commonly Gaussian distributed according to (Jouin et al., 2016)) from the initial state of the system and then implements particle population propagation as per (1) and updates particle weights by means of resampling strategies during the state tracking phase. Several resampling methods exist in the literature, one of which is the sequential importance resampling (SIR) method (T. Li, Bolic, & Djuric, 2015). It has the advantages that the weights are easily evaluated and the density can easily be sampled. In this way, the posterior distribution of the system state represented by the particles can be updated in a step-by-step manner throughout state tracking phase.

To be specific, PF uses a set of random samples with associated weights $\{(x_k^j \pi_k^j); j = 1, 2, 3, ..., N\}$ sampled from a distribution, $q\left(x\right)$ to approximate the posterior marginal density of the system state:

$$p\left(x_k \mid y_{1:k}\right) \approx \sum_{j=1}^{N} \pi_k^j \delta\left(x_k - x_k^j\right) \tag{2}$$

where N is the number of particles, and $\sum_{j=1}^{N} \pi_k^j = 1$. When new measurements become available, particle weights π_k^j are updated accordin to the principle of importance sampling:

$$\pi_k^j \propto \pi_{k-1}^j \cdot \frac{p\left(y_k \mid x_k^j\right) p\left(x_k^j \mid x_{k-1}^j\right)}{q\left(x_k^j \mid x_{k-1}^j, y_k\right)} \tag{3}$$

In the context of using PF for prognostics, where the internal system state is not directly measurable, a canonical representation of the measurement equation can be used:

$$y_k = x_k + v_k \tag{4}$$

where x_k represents the true system state, v_k is a noise term and y_k denotes a one-dimensional health index derived from the system's measurements. (1) - (4) indicate that one can use dimensionality reduction techniques to compute a health index, which represents the true system state v_k, and then use particles to approximate the system state's distribution under the PF framework. When the system's measurements are available, PF implements state tracking during which the particles and weights are updated continuously. Then the state prediction phase is implemented to propogate the existing particles population.

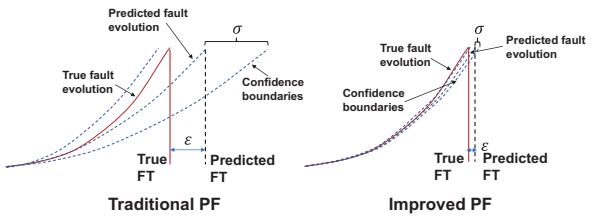

Fig. 1: Comparison between traditional PF and the improved PF in terms of predictive accuracy and uncertainty.

During the state prediction phase, the state evolution model (1), which was trained using the up-to-date observations, projects at future times the current particles population $p\left(x_k \mid y_{1:k}\right)$, without the presence of new measurements. This procedure could be expressed as:

$$p\left(x_{k+h} \mid y_{1:k}\right) = \int \ldots \int \prod_{j=k+1}^{k+h} p\left(x_j \mid x_{j-1:j-4}\right) p\left(x_{k+h} \mid y_{1:k}\right) \prod_{j=k}^{k+h-1} dx_j = \sum_{j=1}^{N} \pi_{k+h-1}^j p\left(x_{k+h} \mid x_{k+h-1:k+h-4}^j\right) \tag{5}$$

where $j = k+1, k+2, \ldots, k+h$ represents the future time instances, $p\left(x_j \mid x_{j-1:j-4}\right)$ denotes the state transition probability and $p\left(x_{k+h} \mid y_{1:k}\right)$ is the h step ahead posterior distribution.

However, it has been pointed out in the literature (Jouin et al., 2016; Xiongzi et al., 2012; Tang, DeCastro, Kacprzynski, Goebel, & Vachtsevanos, 2010; J. Liu, Wang, Ma, Yang, & Yang, 2012) that when PF is used for long-term prognostics, it extrapolates the particles population $p\left(x_k \mid y_{1:k}\right)$ obtained at the end of the state tracking phase along different possible future trajectories, and the following problems may occur: The prediction results greatly depends on the state particles estimated at initial prediction step and their parameters are approximately static (i.e. there is no update of the model parameters during the prediction), which increases the uncertainty; Any errors or approximation in the initial pdf can accumulate and grow over a certain time horizon and can severely distort the predicted pdf over a long time frame, result in a large grain of uncertainty. Therefore, our solution is, the health index found by a similarity matching method will be treated as "new measurements" to realize particles, weights and pdf updates during the state prediction phase. This method allows the PF model parameters to be updated recursively according to the accuracy of prediction, and the particles are regenerated iteratively based on how close they are to the matched HI. As a result, the aforementioned predictive uncertainty and pdf distortions caused by long-term error accumulations can be addressed. Fig.1 illustrates the possible

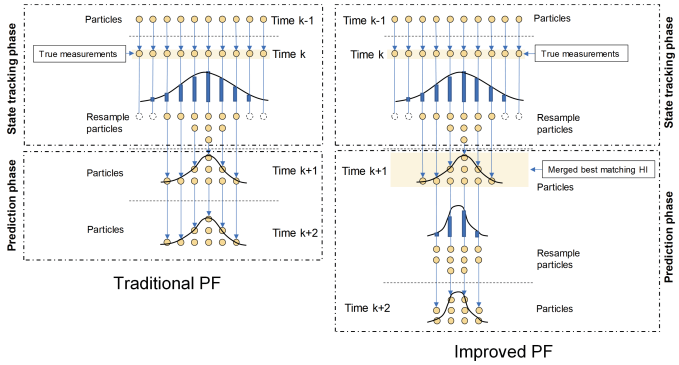

Fig. 2: Conceptual illustration of the difference between traditional PF and the improved PF

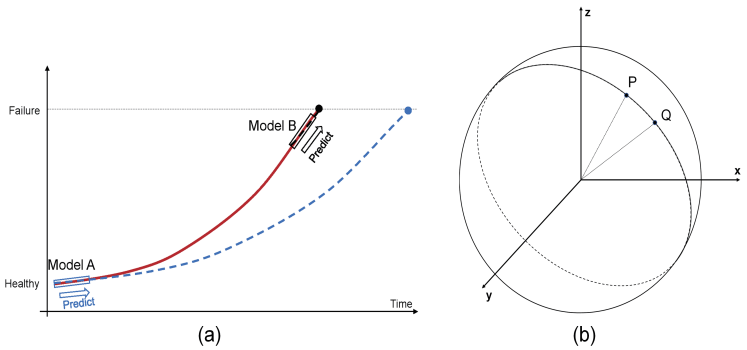

Fig. 3: (a) Illustration of the effects of training data on predictive accuracy. (b) Schematic illustrating the Spherical distance concept.

deficiencies induced by the PF scheme and the improved results after applying our proposed solution. The following section details how the proposed index similarity-assisted PF can address the aforementioned challenges.

III. METHODOLOGY

This Section describes the improved PF that incorporates a novel similarity matching method to enable updates of particles and the associated weights during the prediction phase (see Fig.2 for illustration).

A. Canonical Variate Analysis for HI Construction and Prediction Start Time Determination

Although fault detection is not the main task of this study, it is the starting point for prognostics. Canonical variate analysis (CVA) has been successfully applied to HI construction (X. Li, Yang, Yang, Bennett, & Mba, 2019; X. Li, Yang, Yang, Bennett, Collop, & Mba, 2019) for prognostic purposes previously. In this work, CVA is applied to transform the multidimensional measurements to a single dimensional HI. For further details on CVA for fault detection and prognostic HI construction, readers are referred to (X. Li, Yang, Yang, Bennett, & Mba, 2019; X. Li, Yang, Yang, Bennett, Collop, & Mba, 2019; X. Li, Yang, Bennett, & Mba, 2019).

B. Similarity Matching Based on Spherical Similarity and Cosine Similarity

The calculated HIs are first stored in a training library. Then a similarity matching method can be applied to search for HIs that are similar to the HI of the testing machine. Two similarity criteria - the Spherical similarity and the Cosine similarity - are considered in this work.

1) Spherical Similarity: Index similarity can be evaluated at multiple time stamps, and traditionally the distances calculated at different time instances are allocated with the same weight. Assuming two different prediction models, A and B, are trained using two different portions captured from the same HI. A is trained using data from the very beginning and B is trained using a segment near the end of failure (Fig.3 (a)). Apparently, B is more likely to generate an accurate estimate of the FT since its training data captures the latest degradation trend. In comparison, model A's training data yet to show signs of severe degradation, and the model error inherent in A will be propagated over a long time to the predicted FT, causing inaccurate predictions and large uncertainty. Therefore, when searching for similar HIs in the library, it is reasonable to weight the data higher closer to the end of failure since these data points capture the latest degradation trend and could more likely end up with a failure time which is close to that of the testing machine. To aggregate these similarity levels at different time instances, we define Spherical similarity as a normalized weighted sum of relative similarity at specific time stamps. Suppose the training library has been built and the up-to-date testing HI data $\Delta Z_t = Z_{t,1}, Z_{t,2}, \ldots, Z_{t,N} \in R^N$ is given, the Spherical similarity between ΔZ_t and the relevant data in the library $\Delta Z_r = Z_{r,1}, Z_{r,2}, \ldots, Z_{r,N} \in R^N$ is defined as

$$D_s\left(\Delta Z_t, \Delta Z_r\right) = \sum_{k=1}^{N} w_k E_k \tag{6}$$

$$E_k = \left\| Z_{t,k} - Z_{r,k} \right\| \tag{7}$$

$$w_k = \frac{2}{\pi} \arccos\left(\sqrt{\mu_{k-1}\mu_k} + \sqrt{\left(1-\mu_k\right)\left(1-\mu_{k-1}\right)}\right) \tag{8}$$

where $\mu_k = \mu_l + \frac{k(\mu_h - \mu_l)}{N}, k = 1, 2, \ldots, N$, μ_l and μ_h are the lower and higher boundary for determining the Spherical distance w_k, and $0 < \mu_l < \mu_h < 1$. E_k represents the Euclidean distance between the point, $Z_{t,k}$, on the testing HI and the point, $Z_{r,k}$, on the reference (historical) HI. w_k represents the weight being allocated to the distance between the points $Z_{t,k}$ and $Z_{r,k}$. Spherical distance was first proposed in 2009 (Y. Yang & Chiclana, 2009) to create nonlinear distances with respect to the change of the corresponding fuzzy membership degrees. As shown in Fig.3 (b), the Spherical distance between two consecutive points of a HI is expressed as the spherical distance between their corresponding points (namely P and Q in Fig.3 (b)) on its restricted spherical surface representation. When evaluating the similarity between two HIs, the Spherical similarity adopted in this study assigns

higher weights to points near the FT and vice versa. For further details on Spherical distance, see (Y. Yang & Chiclana, 2009).

2) Cosine Similarity: The Cosine distance, which measures the spatial distances between two vectors, is often neglected by the similarity-based prognostics community (Y. Liu et al., 2019). It is defined as

$$D_c\left(\Delta Z_t, \Delta Z_r\right) = \cos(\varphi) = \frac{\Delta Z_t^{\mathrm{T}} \Delta Z_r}{\|\Delta Z_t\| \, \|\Delta Z_r\|} \tag{9}$$

3) Similarity Matching: A similarity matching method which is based on Spherical and Cosine similarity is proposed to predict the future HI of the system. This method searches for the HI segments $\Delta Z_r \in R^N$, that are similar to the up-to-date HI data $\Delta Z_t \in R^N$ of the testing machine. Each of the matching HI is assigned with a weight w in relation to its Spherical and Cosine similarity, and w is claculated as

$$w = D_s + D_c \tag{10}$$

Where D_c equals $1/D_c\left(\Delta Z_t, \Delta Z_r\right)$. The HI value at a future time $k+h$ is then determined by the weighted sum of all best matching HIs at time $k+h$ (i.e. HIs are merged). The merged HI can then be continuously fed into the PF as new "measurements" during the state prediction phase. The effectiveness of the Spherical-Cosine similarity matching method will be compared with that of the Euclidean distance-based approaches later through experiments.

C. Adjust merged HI Based on Teaching-learning-based Optimization

While the generated "measurements" offer an opportunity to update particle population during prediction, the question arises, whether the merged best matching HI should be considered as more suitable to represent the fault evolution than the standard PF? When the historical failure data are abundant and the merged best matching HI tracks the system degradation accurately, the improved PF would unsurprisingly be able to deliver precise FT predictions. However, occasionally the merged HI could deviate from the actual degradation as shown in Fig.4. This can be attributed to the lack of similar historical HIs in the training library. In order to solve this problem, a TLBO algorithm is adopted in this study to realize a Procrustes analysis, rotating the imperfect HI to make it closer to the actual FT. Procrustes analysis is a form of statistical shape analysis used to superimpose a pair of shape instances through translation, rotation and scaling (Dryden & Mardia, 2016). The goal is to find the optimal rotational angle of the merged HI to realize a closer agreement with the testing HI in that the Spherical and Cosine distances between both HIs are minimized.

Let $\Delta Z_m = Z_{m,1}, Z_{m,2}, \ldots, Z_{m,N} \in R^N$ be the merged best matching HI up to time k. The pseudocode of the proposed Procrustes analysis algorithm is provided below.

1) Teaching-learning-based Optimization: TLBO, as a nature inspired optimization algorithm, has been proven to be more effective than its counterparts due to its fewer setting parameters and computational efficiency (Rao et al., 2011). It has been applied to solve industrial optimization problems in the field of transportation systems (Tian, Zhou, Li, Zhang, & Jia, 2016), low-carbon manufacturing (Lin et al., 2017) and mechanical design problems (Rao et al., 2011), etc. In this study TLBO is adopted to solve the optimization problem mentioned in Algorithm 1 in order to achieve fast determination of the optimal rotational angle $\hat{d}_\theta$. It is also the first known implementation of TLBO in FT prediction.

Algorithm 1 Procrustes Analysis

1: **for** $1 \le k \le N$ **do**
2: $\quad \boldsymbol{x}\left(\Delta Z_m\right) \leftarrow \Delta Z_m, \boldsymbol{y}\left(\Delta Z_m\right) \leftarrow \Delta Z_m$ [a]
3: $\quad \boldsymbol{x}\left(\Delta Z_t\right) \leftarrow \Delta Z_t, \boldsymbol{y}\left(\Delta Z_t\right) \leftarrow \Delta Z_t$
4: $\bar{x}_m = \mathrm{mean}\left(x\left(\Delta Z_m\right)\right), \bar{y}_m = \mathrm{mean}\left(y\left(\Delta Z_m\right)\right)$
5: $\bar{x}_t = \mathrm{mean}\left(x\left(\Delta Z_t\right)\right), \bar{y}_t = \mathrm{mean}\left(y\left(\Delta Z_t\right)\right)$
6: $\boldsymbol{t_x} = \left(\boldsymbol{x}\left(\Delta Z_m\right) - \bar{x}_m\right) \times \left(\cos\left(d_\theta\right) - \sin\left(d_\theta\right)\right) + \bar{x}_m$ [b]
7: $\boldsymbol{t_y} = \left(\boldsymbol{y}\left(\Delta Z_m\right) - \bar{y}_m\right) \times \left(\sin\left(d_\theta\right) + \cos\left(d_\theta\right)\right) + \bar{y}_m$ [c]
8: $\mathbf{Z}_{tr}$ [d] $\leftarrow \left(\boldsymbol{t}_x, \boldsymbol{t}_y\right)$
9: $f\left(d_\theta\right)$ [e] $= D_s\left(\Delta Z_t, \mathbf{Z}_{tr}\right) + D_c\left(\Delta Z_t, \mathbf{Z}_{tr}\right)$ [f]
10: $\hat{d}_\theta$ [g] $= \mathrm{argmin}\left(f\left(d_\theta\right)\right)$, s.t. $d_{\theta,l} \le d_\theta \le d_{\theta,h}$ [h]
11: Subsitute $\hat{d}_\theta$ into steps 6 - 8 to calculate $\mathbf{Z}_{tr,\hat{d}_\theta}$ [i]

[a] $\boldsymbol{x}\left(\cdot\right)$ and $\boldsymbol{y}\left(\cdot\right)$ denote the projections of a vector on the x and y coordinates, respectively.
[b] d_θ is the rotation angle to be optimized.
[c] Steps 6 - 7 realize the rotation of the merged HI ΔZ_m according to the rotational angle d_θ.
[d] $\mathbf{Z}_{tr}$ stores the projections of the rotated merged HI on x and y coordinates, $\boldsymbol{t}_x$ and $\boldsymbol{t}_y$ respectively.
[e] $f\left(d_\theta\right)$ denotes the objective function to be optimized.
[f] $D_s\left(\Delta Z_t, \mathbf{Z}_{tr}\right)$ and $D_c\left(\Delta Z_t, \mathbf{Z}_{tr}\right)$ denote the Spherical and Cosine similarity between the testing and the rotated merged HI, respectively.
[g] $\hat{d}_\theta$ is the optimal rotation angle to be approached.
[h] $d_{\theta,l}$ and $d_{\theta,h}$ are the lower and higher boundaries of the design variable d_θ.
[i] $\mathbf{Z}_{tr,\hat{d}_\theta}$ is the rotated/adjusted HI that can be fed into the subsequent PF analysis.

The process of TLBO consists of a teaching phase and a learning phase. Each learner in the class is a possible solution to the optimization problem and the entire class is a population. Learners learn from the teacher during the teaching phase and learn from other learners through interaction during the learning phase. Steps to implement TLBO are detailed as follows.

a) Objective function and initialization.

As stated in Algorithm 1, the objective function is $f\left(d_\theta\right)$. Furthermore, the size of the population P (i.e. the number of learners), the number of generations G and the lower and upper boundaries of the design variable, $d_{\theta,l}$ and $d_{\theta,h}$, need to be initialized in this step.

b) Teaching Phase.

The best solution in the first iteration will be regarded as the teacher

$$d_{\theta,\text{teacher}} = d_{\theta,f(d_\theta)=\min} \tag{11}$$

At the same time, the teacher will try to shift the population mean $\bar{d}_\theta$ towards its own value $d_{\theta,\text{teacher}}$. The shifted population mean is

$$\bar{d}_{\theta,s} = d_{\theta,\text{teacher}} \tag{12}$$

The difference between the old and the shifted mean is defined as

$$\Delta d_\theta = r\left(\bar{d}_{\theta,s} - T_f \bar{d}_\theta\right) \tag{13}$$

where the value of r is randomly chosen between 0 and 1, and the value of T_f is chosen as 1 or 2 (Rao et al., 2011). This difference is then used to adjust the old mean, and the finally updated new mean is expressed as

$$\bar{d}_{\theta,\text{new}} = \bar{d}_\theta + \Delta d_\theta \tag{14}$$

$\bar{d}_{\theta,\text{new}}$ will be accepted if its corresponding objective function value is smaller than that of the old population mean.

c) Learning Phase. In this step, learners learn from other learners through randomly mutual interactions. A learner gains new knowledge if the other learner is better. For each learner $d_{\theta,i}\,(i = 1:P)$ in the population, randomly select another learner $d_{\theta,j}\,(d_{\theta,i} \neq d_{\theta,j})$, and perform the following calculation

Algorithm 2 Learning Phase

1: **if** $f\left(d_{\theta,i}\right) \leq f\left(d_{\theta,j}\right)$ **then**
2: $\quad d_{\theta,i}^{new} = d_{\theta,i} + r\left(d_{\theta,i} - d_{\theta,j}\right)$
3: **else** $d_{\theta,i}^{new} = d_{\theta,i} + r\left(d_{\theta,j} - d_{\theta,i}\right)$

where $d_{\theta,i}^{new}$ will be accepted if its corresponding objective function value is smaller than that of $d_{\theta,i}$.

d) Termination of Iteration.

The iteration will be terminated when the maximum generation number G is achieved.

TLBO will be employed to determine the optimal rotational angle that the merged HI needed for the FT compensation.

D. Synthesis and FT Prediction

The CVA approach, which is described in Section III-A, is applied to compute the HIs for all machines under study. Then, as described in Section III-B-3), a portion of the testing HI is compared with all the reference HIs in the training library using a similarity measure calculated based on the Spherical and Cosine similarity as described in Section III-B-1) and Section III-B-2), respectively. Then, a merged HI is calculated by a weighted average of the similar HIs found in the library. Subsequently, a TLBO-based Procrustes analysis is adopted to adjust (rotate) the merged HI such that the points of the merged HI can best conform those of the testing HI. This adjustment is achieved through minimizing an objective function of the Spherical and Cosine distance between the merged and the testing HIs. The details of the Procrustes analysis are described in Section III-C. Finally, the adjusted merged HI is continuously fed into the particle filter as new "measurements" after the end of the state tracking phase, and as a result the state prediction phase is implemented in the same way as the state tracking phase. The merged HI consistently updates the particles and their weights to restore

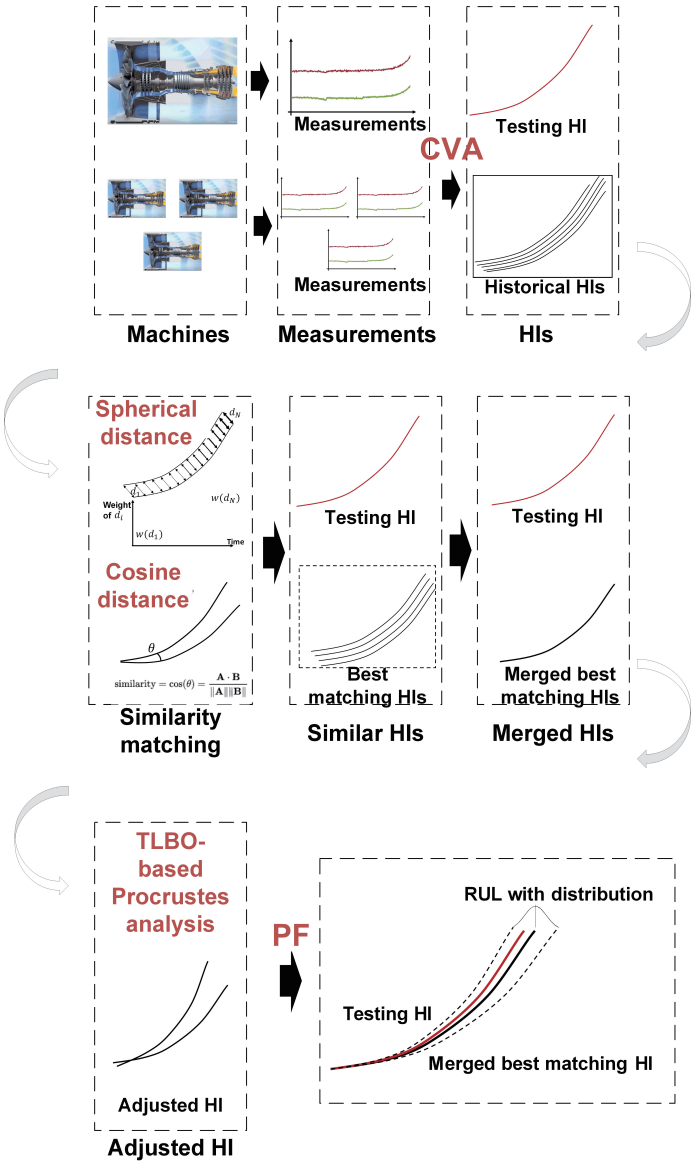

Fig. 4: Flowchart of the improved PF FT prediction algorithm.

them back to reasonable values. The concept of the proposed improved PF FT prediction method is illustrated in Fig.4. Moreover, Fig. 5 specifies the structure of the proposed particle filter prognostic model.

E. Modelling Steps

The proposed index similarity-based particle filter framework for prognostics is summarized as follows, which consists of 4 main steps.

Step 1: Health index construction

Construct health indexes from historical failure measurements as well as the test unit's most recent available measurements according to the CVA algorithm (X. Li, Yang, Yang, Bennett, & Mba, 2019; X. Li, Yang, Yang, Bennett, Collop, & Mba, 2019).

Step 2: Particles initialization

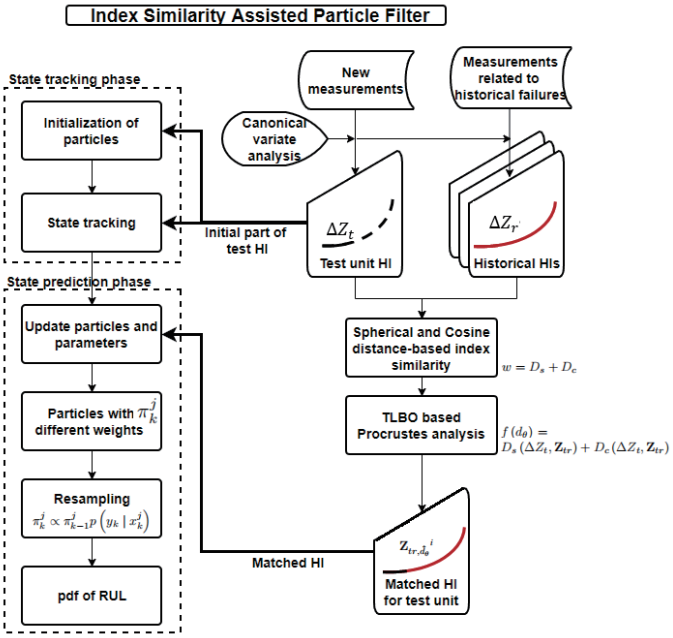

Fig. 5: Structure of the proposed particle filter prognostic model

Generate a set of particles to approximate the posterior distribution of the system state according to the initial value of the HI as per Equation (2)

Step 3: State tracking

(a) Propagate the distribution of the particles according to the state evolution model described in Equation (1)

(b) Update each particle's weight as per Equation (3)

(c) The updated posterior distribution is represented as per Equation (2)

(d) Repeat steps (a) – (c) at each time instance throughout the state tracking phase

Step 4: Index assisted state prediction

(a) Evaluate the Cosine-Spherical similarity between the test unit and past failures' HIs as per Equations (6) – (10) to find the best matching HI

(b) Perform statistical Procrustes analysis as per Equations (11) – (14) and Algorithm 1 to minimize the distance between the test unit' HI and the best matching HI

(c) Draw initial population from the state tracking phase

(d) Project at future times the current particle population without the presence of new observations as per Equation (5)

(e) Update each particle's weight as per Equation (3) according to the deviation from the best matching HI

(f) Repeat steps (d) – (e) at each time instance throughout the state prediction phase

(g) The updated FT posterior distribution is represented as per Equation (2)

IV. CASE STUDY I: TURBOFAN ENGINE DATASETS

A. Description of Dataset I

In this subsection, data generated from the Commercial Modular Aero Propulsion System Simulation (C-MAPSS) program (Ramasso & Saxena, 2014) are presented. The data can be considered to be captured from a fleet of 100 engines of the same type. The data contain 100 multivariate data sets. The engines were operating normally at the start and developed a fault at some point. The fault grew in magnitude until system failure. Similar to (Tidriri, Verron, Tiplica, & Chatti, 2019; Wang et al., 2008), 9 complementary variables among the total 26 variables found in the dataset (corresponding to variables 2, 3, 4, 7, 11, 12, 15, 20 and 21) were selected to construct the HIs.

B. Description of Dataset I

The CVA technique as proposed in (X. Li, Yang, Yang, Bennett, Collop, & Mba, 2019; X. Li, Yang, Yang, Bennett, & Mba, 2019) is applied to calculate the HIs using the selected complementary variables. A time window covering the first 30 hours of operation is extracted from each engine, and theses windows are combined to form the training data of CVA. In other words, each engine is considered to be normal for the first 30 samples, which is in line with the characteristics of the data (Wang et al., 2008). By doing this, the variations of the fleet of machines are fully accommodated, thereby avoiding the excessive amount of false alarms which are frequently encountered by site engineers in practical applications. The upper control limit is determined using the Kernel density estimation method (Odiowei & Cao, 2009) with a 99% confidence level. Similar to (Javed et al., 2014; X. Li, Yang, Yang, Bennett, & Mba, 2019), a locally weighted scatterplot smoothing (LOWESS) with a span value of 30% was employed to smooth the calculated HIs. The prediction start times are determined when the calculated HI exceeds the control limit.

C. Whether the HIs Resulted from the Proposed Similarity Matching Method Are Better Than Those from Other Similarity Matching Methods?

After the HIs are constructed and the prediction start times are determined, the similarity matching method as proposed in Section III-B is used to calculate the merged best matching HI for each of the testing engines. Euclidean distance-based similarity and Cosince-similarity has been widely used for similarity-based prognostics. The question arises, whether the merged HIs resulted from the proposed combined Spherical and Cosine similarity should be considered as more reliable and suitable for prognostics with respect to Euclidean, Spherical and Cosine similarity? To solve this problem, we define a criterion to evaluate the suitability of the merged HIs for predicting failure time.

$$I = \left| k_{th}^{|d|} - k_{th} \right| \tag{15}$$

In (15), k_{th} is the time when the testing HI reaches its failure point (i.e. the true failure time(FT)). $k_{th}^{|d|}$ is the time when the calculated HI reaches the failure threshold, where $|d|$ denotes the corresponding similarity method. A calculated HI that is closer to the actual FT k_{th} when it reaches the failure threshold should be considered as more desirable for RUL prediction.

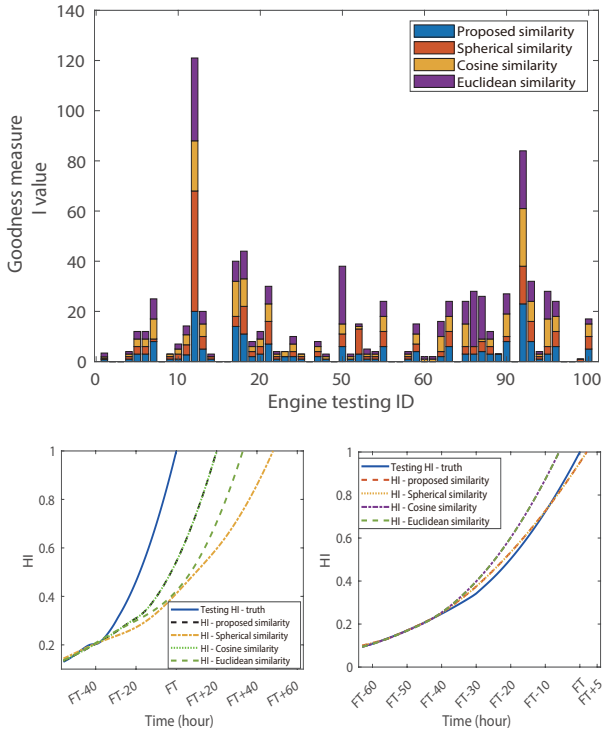

Fig. 6: Upper: HI Estimation error over all testing engines. Lower: Demonstration of HIs obtained using the proposed similarity and its counterparts. Lower left: engine no. 12; Lower right: engine no. 42.

The criterion I in (15) indicates how far the "FT" of the HI (calculated using the corresponding similarity method) is from the actual FT. I is suitable for RUL prediction when its value is small. The values of I for all 60 testing engines are illustrated in Fig. 6 (Upper). It is worth noting that engines no. 1-20, 41-60 and 81-100 (total 60 engines) are randomly and evenly selected from the 100 units as testing engines. The lower and upper bound for Spherical distance were determined using grid search and were set to 0.5 and 0.6, respectively. It is obvious that for most of the cases studied, the merged HI computed using the proposed similarity matching method is more suitable for FT prediction compared with Euclidean, Spherical and Cosine similarity, with Euclidean similarity being the worst. The averaged I value for the proposed combined similarity, Euclidean, Spherical and Cosine similarity are 3.25, 4.31, 3.31 and 3.4 hour, respectively, meaning that the proposed similarity is collectively better than its counterparts in terms of finding the suitable HIs for subsequent PF analysis. We observed that through parameter tunning, Spherical distance shows promising resultes for finding suitable HIs for prognostics than other 'model-fixed' distance measures, mainly due to its ability to see the similarity at each time point with a different weight.

Fig. 6 (Lower) demonstrates two exemplary results of the HIs calculated using the proposed combined similarity and other similarity methods for case no. 12 and no. 42, respectively. These two examples demonstrate that the combined similarity leverages the strength of Spherical and Cosine similarity, yielding collectively better HIs that are closer to the actual FT when they reache the failure threshold.

D. FT prediction and Discussion

The TLBO-based Procrustes analysis as described in Section III-C was utilized to rotate the potentially imperfect merged HI to best conform its points to those of the testing HI. In this way, the predictive accuracy of the proposed prognostic framework can be further improved. The lower and higher boundaries of the rotational angle d_θ, $d_{\theta,l}$, and $d_{\theta,h}$were set to 0 and 90 degrees respectively (-90 and 0 when the HI needs to be rotated anticlockwise) because all HIs lie in the first quadrant of the x-y coordinates. The size of the population P and the number of generations G were set to 200 and 200, respectively. Each TLBO was executed for 30 times and the optimal angle $\hat{d}_\theta$ was taken as the mean value of the 30 runs. To ensure a fair comparison, similar to (J. Wu et al., 2018), the state evolution model was selected as exponential regression for both the proposed and the standard PF. Fig. 7 (a) upper subplot is an exemplary result of the TLBO-based Procrustes analysis where the blue curve shows the original merged HI, and the red curve shows the actual HI (engine no. 7).

Given the HI values up to time instance FT-28, the TLBO method finds the optimal rotational angle, moving the "predicted FT" at least 8 hours closer to the actual FT. Fig. 7 (a) lower subplot demonstrates the resultant FT predictions for predictions starting at different times. In this case, FT-60 is the initial prediction start time determined by the CVA method. Then the data from FT-60 up to the current time are used to train the prognostic framework following the steps described in Sections III-B - III-D. The areas between the dashed black curves denote the one sigma tolerance interval with particles being assumed normally distributed. It is observable from the figure that the predictive accuracy of the standard PF method is lower at the beginning, and the predicted FT gets closer to the true FT over time. In comparison, the predicted failure time using the proposed method is not only centered closer to the actual FT at all times but also has narrower confidence boundaries, especially at early degradation stages. Furthermore, using the HI curve from early cycles yet to exhibit severe performance degradation, we applied the proposed prognostic approach to precisely predict the failure time, earning ample time to plan future missions. The standard PF requires at least 40 hours of training data before making estimations at a precision comparable to that of our method. This example highlights the promise of combining similarity-based prognostics and Procrustes analysis to predict the behaviour of complex rotating machines. Fig. 7 (b) shows an exemplary result for the prognostic results of engine no. 60. The upper subplot shows the testing HI (red) and the adjusted merged HI obtained through TLBO at time FT-50 (blue). Since the original merged HI already shows close agreement with the testing HI, the optimal rotational angle calculated is near zero after executing the Procrustes analysis. The lower subplot shows the predicted FT for predictions starting at different time instances.

Analysis was carried out to assess the prognostic performance of the proposed PF on all 60 testing engines in terms

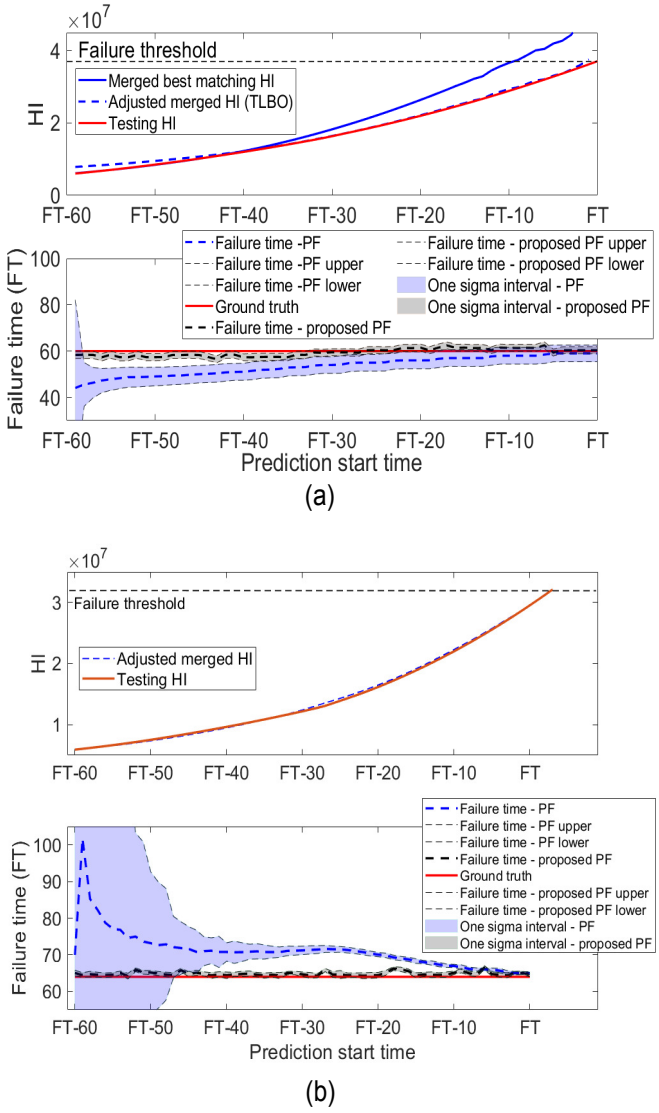

Fig. 7: (a) Exemplary prognostic results for engine no. 7. Upper: results of TLBO at time FT-28. Lower: failure time estimation for predictions starting at difference times. (b) Exemplary prognostic results for engine no. 60. Upper: results of TLBO at time FT-50. Lower: failure time estimation for predictions starting at difference times.

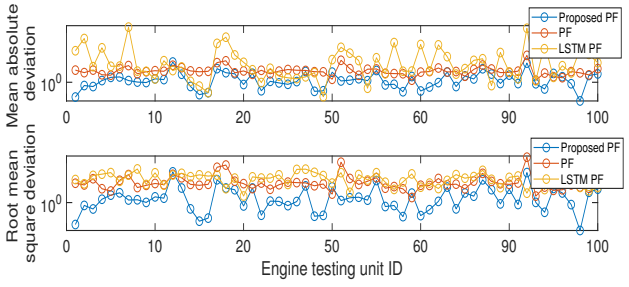

Fig. 8: Performance of the proposed PF on all test instances

of predictive accuracy. As shown in Fig. 8, the proposed PF has achieved a higher predictive accuracy for most of the testing engines. We compared our proposed PF (with Procrustes

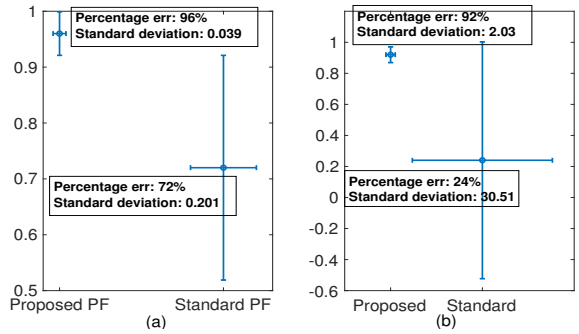

Fig. 9: Predictive performance (percentage error) using early-cycle HI data. (a) C-MAPSS data; (b) Compressor valve data.

analysis) with three other methods: the proposed PF without Procrustes analysis, the standard PF and the standard PF with long-short term memory (LSTM). It is worth noting that LSTM is a famous and powerful prediciton algorithm particularly suitable for time series prediction, and it has previously been utilized for remaining useful life prediction (J.-Y. Wu, Wu, Chen, Li, & Yan, 2021; X. Li, Duan, Loukopoulos, Bennett, & Mba, 2018). In the comparison, LSTM was employed as a predictor to predict the future evolution of HI trajectories. The number of layers, number of units and learning rate of the LSTM network were determined through a grid search process. To numerically assess the results, the averaged MAE and RMSE over all testing engines were calculated, see Table I. The errors of the proposed PF but without Procrustes analysis is higher when compared with the proposed PF with TLBO-based Procrustes analysis, highlighting the importance of employing Procrustes analysis to accommodate prediction errors caused by unexpected imperfect merged HIs. It is worth noting that, in case study I, the prediction errors of the LSTM PF are the largest. This is mainly due to the reason that LSTM was not able to precisely predict the fault evolution relying on limited training data when compared with our proposed PF, leading to consistent in accurate HI prediction (see Fig. 10). In Fig.10, the predicted trajectories consisting of particles generated using LSTM-PF and Spherical-Cosine similarity PF method were demonstrated, and the predictions were made at different times. Obviously, LSTM was not able to achieve an accuracy that was comparable to our proposed method. Additional analysis was performed to assess the predictive performance when early-cycle HI data are used. The proposed PF achieved an averaged accuracy of 96% when only 10% of the degradation data were used. In comparison, the average percentage error for the standard PF was 72% (see Fig. 9 (a)). It is worth noting that the error bar, which represents the one standard deviation of uncertainty, associated with the proposed PF (0.039) is much smaller than that of the standard PF (0.201), indicating that our method can reliably provide more precise FT estimates.

V. CASE STUDY II: COMPRESSOR VALVE FAILURE DATASETS

The second dataset used in this paper was captured from a two-stage, four-cylinder, double-acting operational reciprocat-

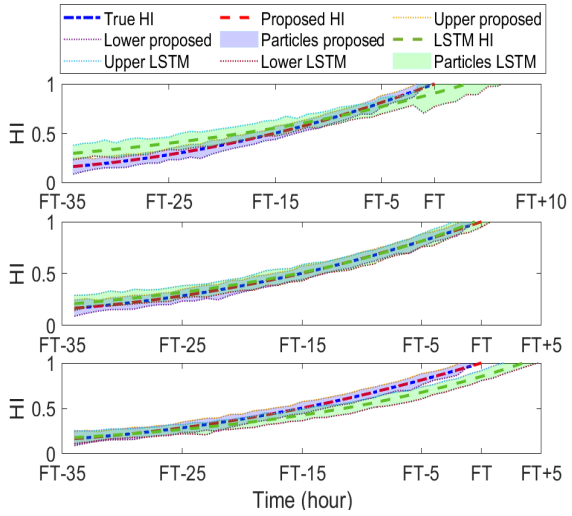

Fig. 10: Illustration of the proposed similarity method and LSTM's performance on RUL prediction for case no. 81. Shaded areas consist of particles generated using LSTM PF and the proposed PF, and predictions were made at different times.

TABLE I: COMPARISON OF PREDICTIVE ACCURACY

Metrics	MAE	RMSE
Proposed PF	2.17	2.38
Proposed PF without Procrustes analysis	3.24	3.30
Standard PF	5.89	7.97
LSTM PF	8.04	9.67

∗ All results were averaged across all 60 testing engines.

TABLE II: COMPARISON OF PREDICTIVE ACCURACY

Metrics	MAE	RMSE
Proposed PF	6.64	7.17
Proposed PF without Procrustes analysis	7.85	8.05
Standard PF	24.2	28.1
LSTM PF	7.61	7.66

∗ All results were averaged across all 11 failure cases.

ing compressor. The machine experienced eleven valve failures within a period of 18 months with all failures took place at the fourth cylinder. The root cause of these failures was found to be improper sealing of the valve due to a missing piece from the outer structure of valve plate. These failures occurred at either the head end (HE) or the crank end (CE) discharge valve. Only temperature measurements were recorded by the monitoring system. Eight temperature ratios, namely Suction temperature HE/CE cylinder 1-4 and Discharge temperature HE/CE cylinder 1-4 were utilized by the site engineer for monitoring the health status of the valves.

The CVA technique is applied to calculate the HIs using the eight temperature ratios. Furthermore, a time window covering the first 10 steps of operation is extracted from each failure case, and theses windows are combined to calculate the upper control limit for determining the prediction start time. Fig. 11 illustrates the resultant HIs after the prediction start time was determined for all 11 failure cases. Since the HIs demonstrate the highly desirable characteristic of having very similar values

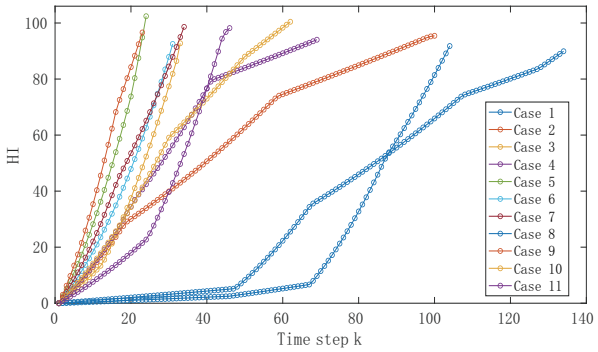

Fig. 11: Fault evolution for failure cases 1-11

at the end of fault evolution, the failure threshold was set to 91.

Failure times demonstrate individual variations between failure cases highlighting the stochastic nature of fault evolution in real-world applications. These variations were mainly caused by the different applications the compressor was used (the machine compressed various gases). Individual variations and limited amount of failure cases (11 failure cases in total) have made forecasting the FT of this machine a complicated challenge. We thereby use this dataset to test the generality and superiority of the proposed method.

To ensure a fair comparison, the state evolution model in this case study was selected as polynomial regression for both the proposed and the standard PF. The order of the polynomial regression was determined based on trial and error and was set to three. A general guide is that the fitted curve should both captures the global trend and reflects local variations (Liao, 2013). To appreciate the performance of the proposed method, sample prognostic results for failure case 2 are shown in Fig. 12. The upper subplot shows the testing HI (red) and the adjusted merged HI obtained through TLBO at time FT-87 (blue). Since the original merged HI already shows close agreement with the testing HI, the optimal rotational angle calculated is near zero after executing the Procrustes analysis. The lower subplot shows the predicted FT for predictions starting at different time instances. The FT predicted by the standard PF is seen to be inaccurate when there are only limited failure data available for training. The resultant FT predictions centered closer to the actual FT with a later starting point of prediction. This is due to the amount of failure data is increasing. In comparison, the FT predicted using the proposed method is centered closer to the actual FT at all times. The standard PF requires at least 37 units of training data before making estimations at an accuracy level comparable to that of our method. Moreover, the proposed PF method has narrower confidence boundaries throughout the entire degradation process, and this is due to the "merged HI" which acted as true measurements to update the particles and their weights, thereby reducing the uncertainty of the long-term prediction made by the PF.

Fig. 13 (a)-(b) demonstrate the MAE and RMSE levels of the proposed PF method when compared with the standard PF and LSTM PF for all 11 failure cases. Table II numerically

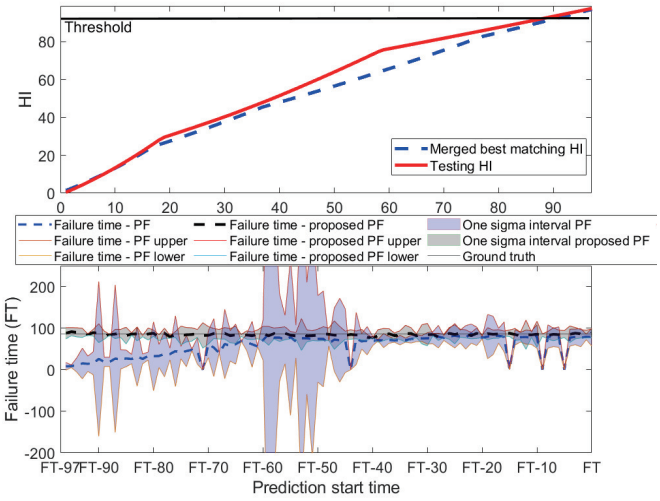

Fig. 12: Exemplary prognostic results for failure case 2. Upper: results of TLBO at time FT-87. Lower: failure time estimation for predictions starting at difference times.

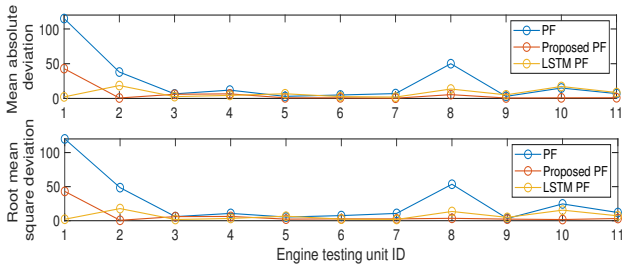

Fig. 13: Performance of the proposed PF on 11 failure cases

summarizes the MAE and RMSE averaged across all 11 compressor failure cases. It is evident that the proposed PF outperforms the standard PF and LSTM PF in terms of predictive accuracy. This can be attributed to the "adjusted merged HI" calculated by the novel similarity-based prognosis method, which not only actually guides the predictions made at different times towards the true failure time but also allows continuous update of particles during long-term prediction. Comparing the first and the second row of Table II, it can be concluded that the merged HI found by Procrustes analysis resulted in the predictions that are closer towards the true failure time when compared with the one without Procrustes analysis. To assess the predictive performance when early-cycle HI data are used, we use only the first 10% of the HI data to train the proposed PF method and achieved an averaged accuracy of 92%, which is similar to the results that we obtained from the turbofan simulation data. In comparison, the average percentage error for the standard PF was only 24% (see Fig. 9 (b)). The one standard deviation associated with the proposed PF (2.03) is also much smaller than that of the standard PF (30.51). The proposed method realized precise early fault prognosis using limited amount of early cycle data, which again highlights the promise of combining similarity-based prognosis and PF to estimate the behavior of real-world complex systems.

VI. CONCLUSIONS

A new index similarity-based particle filter (PF) method was proposed for system failure time (FT) prediction. A novel Spherical and Cosine distance-based index similarity is incorporated into the PF framework, where degradation trajectories found from historical measurements are used to provide estimates of RUL in the form of a probability density function (pdf). To ensure accurate predictions, a Procrustes analysis based on teaching-learning-based optimization (TLBO) was put forward to complement the proposed similarity-based prognostic method when needed. The proposed method was verified on a widely used C-MAPSS engine failure simulation dataset as well as monitoring data captured from a compressor operating in real-world. The advantages of the proposed PF method are summarized as follows. Due to the model parameter updates provided by the similarity-based prognostics, the proposed method offers the promise of improving the predictive accuracy and uncertainty level of the standard PF. The proposed method was also compared with its counterparts in terms of predictive accuracy, and the results showed superior performance over other prognostic models. Additionally, owing to the similarity-based prognostics' ability in assuring long-term prediction, the proposed method shows promise in FT estimation with an early starting point of prediction, making the method a promising tool for early fault prediciton and early maintenance decision making. When then method was tested on simulation and industrial data, we obtained a prognostic accuracy of 96% and 92%, respectively, using only the first 10% cycles. Collectively, this study highlights the promise of combining index similarity, Procrustes analysis and particle filter for developing condition monitoring systems for complex machines such as turbofan engines and compressors.

REFERENCES

Baraldi, P., Cadini, F., Mangili, F., & Zio, E. (2013). Model-based and data-driven prognostics under different available information. *Probabilistic Engineering Mechanics*, *32*, 66–79.

Chen, C., Zhang, B., Vachtsevanos, G., & Orchard, M. (2010). Machine condition prediction based on adaptive neuro–fuzzy and high-order particle filtering. *IEEE Transactions on Industrial Electronics*, *58*(9), 4353–4364.

Chen, N., & Tsui, K. L. (2013). Condition monitoring and remaining useful life prediction using degradation signals: Revisited. *IIE transactions*, *45*(9), 939–952.

Cheng, F., Qu, L., & Qiao, W. (2017). Fault prognosis and remaining useful life prediction of wind turbine gearboxes using current signal analysis. *IEEE Transactions on Sustainable Energy*, *9*(1), 157–167.

Cui, L., Li, W., Wang, X., Zhao, D., & Wang, H. (2022). Comprehensive remaining useful life prediction for rolling element bearings based on time-varying particle filtering. *IEEE Transactions on Instrumentation and Measurement*.

Cui, L., Wang, X., Wang, H., & Ma, J. (2019). Research on remaining useful life prediction of rolling element bearings based on time-varying kalman filter. *IEEE Transactions on Instrumentation and Measurement*, *69*(6), 2858–2867.

Dryden, I. L., & Mardia, K. V. (2016). *Statistical shape analysis: with applications in r* (Vol. 995). John Wiley & Sons.

Hedrea, E.-L., Precup, R.-E., Roman, R.-C., & Petriu, E. M. (2021). Tensor product-based model transformation approach to tower crane systems modeling. *asian journal of control*, *23*(3), 1313–1323.

HEDREA, R.-C. R., & PETRIU, E. M. (2021). Evolving fuzzy models of shape memory alloy wire actuators. *SCIENCE AND TECHNOLOGY*, *24*(4), 353–365.

Javed, K., Gouriveau, R., Zerhouni, N., & Nectoux, P. (2014). Enabling health monitoring approach based on vibration data for accurate prognostics. *IEEE Transactions on industrial electronics*, *62*(1), 647–656.

Jha, M. S., Dauphin-Tanguy, G., & Ould-Bouamama, B. (2016). Particle filter based hybrid prognostics for health monitoring of uncertain systems in bond graph framework. *Mechanical Systems and Signal Processing*, *75*, 301–329.

Jouin, M., Gouriveau, R., Hissel, D., Péra, M.-C., & Zerhouni, N. (2016). Particle filter-based prognostics: Review, discussion and perspectives. *Mechanical Systems and Signal Processing*, *72*, 2–31.

Lei, Y., Li, N., Guo, L., Li, N., Yan, T., & Lin, J. (2018). Machinery health prognostics: A systematic review from data acquisition to rul prediction. *Mechanical systems and signal processing*, *104*, 799–834.

Li, N., Lei, Y., Lin, J., & Ding, S. X. (2015). An improved exponential model for predicting remaining useful life of rolling element bearings. *IEEE Transactions on Industrial Electronics*, *62*(12), 7762–7773.

Li, T., Bolic, M., & Djuric, P. M. (2015). Resampling methods for particle filtering: classification, implementation, and strategies. *IEEE Signal processing magazine*, *32*(3), 70–86.

Li, X., Duan, F., Loukopoulos, P., Bennett, I., & Mba, D. (2018). Canonical variable analysis and long short-term memory for fault diagnosis and performance estimation of a centrifugal compressor. *Control Engineering Practice*, *72*, 177–191.

Li, X., Yang, X., Yang, Y., Bennett, I., Collop, A., & Mba, D. (2019). Canonical variate residuals-based contribution map for slowly evolving faults. *Journal of Process Control*, *76*, 87–97.

Li, X., Yang, X., Yang, Y., Bennett, I., & Mba, D. (2019). A novel diagnostic and prognostic framework for incipient fault detection and remaining service life prediction with application to industrial rotating machines. *Applied Soft Computing*, *82*, 105564.

Li, X., Yang, Y., Bennett, I., & Mba, D. (2019). Condition monitoring of rotating machines under time-varying conditions based on adaptive canonical variate analysis. *Mechanical Systems and Signal Processing*, *131*, 348–363.

Liao, L. (2013). Discovering prognostic features using genetic programming in remaining useful life prediction. *IEEE Transactions on Industrial Electronics*, *61*(5), 2464–2472.

Lim, P., Goh, C. K., Tan, K. C., & Dutta, P. (2017). Multimodal degradation prognostics based on switching kalman filter ensemble. *IEEE transactions on neural networks and learning systems*, *28*(1), 136–148.

Lin, W., Yu, D., Zhang, C., Zhang, S., Tian, Y., Liu, S., & Luo, M. (2017). Multi-objective optimization of machining parameters in multi-pass turning operations for low-carbon manufacturing. *Proceedings of the Institution of Mechanical Engineers, Part B: Journal of Engineering Manufacture*, *231*(13), 2372–2383.

Liu, J., Wang, W., Ma, F., Yang, Y., & Yang, C. (2012). A data-model-fusion prognostic framework for dynamic system state forecasting. *Engineering Applications of Artificial Intelligence*, *25*(4), 814–823.

Liu, Y., Hu, X., & Zhang, W. (2019). Remaining useful life prediction based on health index similarity. *Reliability Engineering & System Safety*, *185*, 502–510.

Liu, Z., Wang, Q., Song, C., & Cheng, Y. (2017). Similarity-based difference analysis approach for remaining useful life prediction of gaas-based semiconductor lasers. *IEEE Access*, *5*, 21508–21523.

Loukopoulos, P., Zolkiewski, G., Bennett, I., Sampath, S., Pilidis, P., Duan, F., ... Mba, D. (2019). Reciprocating compressor prognostics of an instantaneous failure mode utilising temperature only measurements. *Applied Acoustics*, *147*, 77–86.

Loukopoulos, P., Zolkiewski, G., Bennett, I., Sampath, S., Pilidis, P., Li, X., & Mba, D. (2019). Abrupt fault remaining useful life estimation using measurements from a reciprocating compressor valve failure. *Mechanical Systems and Signal Processing*, *121*, 359–372.

Moghaddasi, S. S., & Faraji, N. (2020). A hybrid algorithm based on particle filter and genetic algorithm for target tracking. *Expert Systems with Applications*, *147*, 113188.

Odiowei, P.-E. P., & Cao, Y. (2009). Nonlinear dynamic process monitoring using canonical variate analysis and kernel density estimations. *IEEE Transactions on Industrial Informatics*, *6*(1), 36–45.

Paroissin, C. (2015). Inference for the wiener process with random initiation time. *IEEE Transactions on Reliability*, *65*(1), 147–157.

Qiu, M., Li, W., Jiang, F., & Zhu, Z. (2018). Remaining useful life estimation for rolling bearing with sios-based indicator and particle filtering. *Ieee Access*, *6*, 24521–24532.

Ramasso, E., & Saxena, A. (2014). Performance benchmarking and analysis of prognostic methods for cmapss datasets. *International Journal of Prognostics and Health Management*, *5*(2), 1–15.

Rao, R. V., Savsani, V. J., & Vakharia, D. (2011). Teaching–learning-based optimization: a novel method

for constrained mechanical design optimization problems. *Computer-aided design*, *43*(3), 303–315.

Razavi-Far, R., Chakrabarti, S., Saif, M., & Zio, E. (2019). An integrated imputation-prediction scheme for prognostics of battery data with missing observations. *Expert Systems with Applications*, *115*, 709–723.

Romeo, L., Loncarski, J., Paolanti, M., Bocchini, G., Mancini, A., & Frontoni, E. (2020). Machine learning-based design support system for the prediction of heterogeneous machine parameters in industry 4.0. *Expert Systems with Applications*, *140*, 112869.

Tang, L., DeCastro, J., Kacprzynski, G., Goebel, K., & Vachtsevanos, G. (2010). Filtering and prediction techniques for model-based prognosis and uncertainty management. In *2010 prognostics and system health management conference* (pp. 1–10).

Tang, L., Orchard, M. E., Goebel, K., & Vachtsevanos, G. (2011). Novel metrics and methodologies for the verification and validation of prognostic algorithms. In *2011 aerospace conference* (pp. 1–8).

Teo, A.-C., Tan, G. W.-H., Ooi, K.-B., & Lin, B. (2015). Why consumers adopt mobile payment? a partial least squares structural equation modelling (pls-sem) approach. *International Journal of Mobile Communications*, *13*(5), 478–497.

Tian, G., Zhou, M., Li, P., Zhang, C., & Jia, H. (2016). Multiobjective optimization models for locating vehicle inspection stations subject to stochastic demand, varying velocity and regional constraints. *IEEE Transactions on Intelligent Transportation Systems*, *17*(7), 1978–1987.

Tidriri, K., Verron, S., Tiplica, T., & Chatti, N. (2019). A decision fusion based methodology for fault prognostic and health management of complex systems. *Applied Soft Computing*, *83*, 105622.

Wang, T., Yu, J., Siegel, D., & Lee, J. (2008). A similarity-based prognostics approach for remaining useful life estimation of engineered systems. In *2008 international conference on prognostics and health management* (pp. 1–6).

Wu, J., Wu, C., Cao, S., Or, S. W., Deng, C., & Shao, X. (2018). Degradation data-driven time-to-failure prognostics approach for rolling element bearings in electrical machines. *IEEE Transactions on Industrial Electronics*, *66*(1), 529–539.

Wu, J.-Y., Wu, M., Chen, Z., Li, X.-L., & Yan, R. (2021). Degradation-aware remaining useful life prediction with lstm autoencoder. *IEEE Transactions on Instrumentation and Measurement*, *70*, 1–10.

Wu, Z., Zhang, H., Guo, J., Ji, Y., & Pecht, M. (2022). Imbalanced bearing fault diagnosis under variant working conditions using cost-sensitive deep domain adaptation network. *Expert Systems with Applications*, 116459.

Xiongzi, C., Jinsong, Y., Diyin, T., & Yingxun, W. (2012). A novel pf-lssvr-based framework for failure prognosis of nonlinear systems with time-varying parameters. *Chinese Journal of Aeronautics*, *25*(5), 715–724.

Yang, X., Fang, Z., Yang, Y., Mba, D., & Li, X. (2019). A novel multi-information fusion grey model and its application in wear trend prediction of wind turbines. *Applied Mathematical Modelling*, *71*, 543–557.

Yang, Y., & Chiclana, F. (2009). Intuitionistic fuzzy sets: spherical representation and distances. *International Journal of Intelligent Systems*, *24*(4), 399–420.

Yu, W., Kim, I. Y., & Mechefske, C. (2020). An improved similarity-based prognostic algorithm for rul estimation using an rnn autoencoder scheme. *Reliability Engineering & System Safety*, *199*, 106926.

Zhang, Q.-b., Wang, P., & Chen, Z.-h. (2019). An improved particle filter for mobile robot localization based on particle swarm optimization. *Expert Systems with Applications*, *135*, 181–193.

Zhang, S.-J., Kang, R., & Lin, Y.-H. (2021). Remaining useful life prediction for degradation with recovery phenomenon based on uncertain process. *Reliability Engineering & System Safety*, *208*, 107440.